Journal of the Korean Nuclear Society
Volume 33, Number 5, pp.468~482, October, 2001

An Assessment on the Containment Integrity of Korean Standard Nuclear Power Plants Against Direct Containment Heating Loads

Kyung-Woo Seo and Moo-Hwan Kim
Pohang University
31 San, Hyo-Ja Dong, Nam Gu, Po-Hang City, Kyung-Sang Do, 790-784, Korea
Byung-Chul Lee
Korea Power Engineering Company, Inc.
360-9 Ma-Buk Ri, Gu-Sung Myun, Yong-In City, Kyung-Gi Do, 449-840, Korea
Gyoo-Dong Jeun
Hanyang University
17 Haeng-Dang Dong, Seong-Dong Ku, Seoul, 133-791, Korea
magyna@chosun.ac.kr
(Received March 15, 2001)

Abstract

As a process of Direct Containment Heating (DCH) issue resolution for Korean Standard Nuclear Power Plants (KSNPs), a containment load/strength assessment with two different approaches, the probabilistic and the deterministic, was performed with all plant-specific and phenomena-specific data. In case of the probabilistic approach, the framework developed to support the Zion DCH study, Two-Cell Equilibrium (TCE) coupled with Latin Hypercubic Sampling (LHS), provided a very efficient tool to resolve DCH issue. In case of the deterministic approach, the evaluation methodology using the sophisticated mechanistic computer code, CONTAIN 2.0 was developed, based on findings from DCH-related experiments or analyses. For three bounding scenarios designated as Scenarios V, Va, and VI, the calculation results of TCE/LHS and CONTAIN 2.0 with the conservatism or typical estimation for uncertain parameters, showed that the containment failure resulted from DCH loads was not likely to occur. To verify that these two approaches might be conservative, the containment loads resulting from typical high-pressure accident scenarios (SBO and SBLOCA) for KSNPs were also predicted. The CONTAIN 2.0 calculations with boundary and initial conditions from the MAAP4 predictions, including the sensitivity calculations for DCH phenomenological parameters, have confirmed that the predicted containment pressure and temperature were much below those from these two approaches, and, therefore, DCH issue for KSNPs might be not a problem.

Key Words : high pressure melt ejection (HPME)/direct containment heating (DCH), TCE/LHS, CONTAIN2.0 containment load/strength assessment

1. Introduction

By directly transferring large quantities of the energy from the ejected corium into the containment atmosphere when the reactor pressure vessel (RPV) fails at high system pressure under severe accidents, the containment may be pressurized to a point that the failure is possible. This issue, called as direct containment heating (DCH) resulting from high-pressure melt ejection (HPME), has been of considerable concern to the present design of PWRs and, in consequence, mitigation features have been factored into regulatory and utility requirements such as SECY-93-087 [1] and the Korean Utility Requirements Document (KURD)[2] for the advanced reactor licensing basis. Furthermore, operating plants are deemed to cope with a resolution of this issue in compliance with these requirements, although a choice of practical provision may be limited.

Relying on plant design and accident management strategy, the DCH issues are being approached from four different perspectives [1,2]: depressurization through accident management guidance or recognition of spontaneous depressurization resulting from hot leg creep rupture, in-vessel retention through accident management program, containment load/strength evaluations, or fully integrated level 2 probabilistic safety analysis. While the first two relate to the safety design features and the development of severe accident management guidelines, the last two can be assessed by considering the postulated accident scenarios using some computational tools. Although the DCH issue resolution can be demonstrated by just one of the perspectives, recent licensing process tends to require a defense-in-depth through multiple perspectives. For Korean Standard Nuclear Power Plants (KSNPs), as the first perspective, safety depressurization system (SDS) was adapted in order to reliably depressurize the RCS before the reactor vessel breach (VB). For others, however, there had been no attempt of full-scale on account of insufficient technical development or regulatory requirement yet. If more additional perspective, therefore, needs to be considered, most available choice at present may be containment load/strength evaluations since numerical tools for this work have been well developed.

For containment load/strength evaluations, it can be categorized into two different approaches: deterministic and probabilistic. On the probabilistic approach, the framework developed by M.M. Pilch [3], et al. in support of Zion DCH study provided very efficient tool to resolve DCH issue. This methodology has been applied for all US PWRs [3-7] and one of the conclusions was that most of the plants analyzed, especially including KSNPs like had satisfied the screening criterion established by the methodology and therefore DCH was considered as resolved and no additional analyses were required. Recently, the methodology was applied for the Korean Next Generation Reactor (KNGR) [8]. On the deterministic approach, based on findings from HPME/DCH-related experiments or analyses, the sophisticated mechanistic computer code can be used. The computer code, CONTAIN 1.2 [9] and CONTAIN 2.0[10], maybe unique, can be applied to full-scale plant simulations in which initial and boundary conditions at vessel breach such as RCS thermal hydraulics, core melt mass and composition, etc., have to be derived from other computer codes simulating the RCS meltdown. However, until now the code applications, except for one [11], were based upon the best estimates for expected high-pressure accident scenarios, not focusing on DCH-induced containment loads.

This study is aimed at developing the methodology for containment load/strength evaluation based upon both deterministic and

probabilistic approaches, and, as a result, presenting assessment results as a process to resolve DCH issue for KSNPs. The boundary and initial conditions for two approaches are quantified from US NRC' s DCH study for the bounding scenarios and MAAP4 [12] calculation results for typical plant-specific high-pressure accident scenarios. The sensitivity study for DCH phenomenological parameters is also performed to consider the uncertainties on containment loads so that the assessment results can ensure the containment integrity against DCH threat. General methodology for each approach is described in Section 2. As main part of this study, Section 3 provides the initial and boundary conditions for DCH evaluation and Section 4 presents approach-specific DCH modeling and discusses the calculation results.

2. Methodology

A DCH phenomenon is only of concern if the RPV fails while the RCS is still at elevated pressure. Considering this circumstance, three scenarios selected in previous works of probabilistic approach [3-7] since Zion DCH study sufficiently provide bounding ones for this study. These scenarios, which are designated as Scenarios V, Va, and VI, simulate core melt accidents via small break LOCAs that progress with water still present in the lower portions of the core. In these scenarios, in order to induce HPME/DCH at vessel breach, operator actions are assumed to repressurize the RCS by refilling the RPV with water. Scenario V and Va simulate the RCS repressurization to nearly its overpressure set point, whereas Scenario VI simulates to half an overpressure set point as the consequence of partial operator intervention. Core melt progression and containment thermodynamic conditions for all the scenarios are assumed to be TMI-like accidents, but containment atmosphere for Scenario V and VI differs from TMI-II accident where fan coolers were operational so that there was essentially no steam in the containment. Containment pressure, temperature, and atmosphere composition for Scenario Va are consistent with TMI. On the other hand, in order to verify the conservatism of bounding scenarios and predict the uncertainty of DCH-induced containment loads, typical plant-specific high-pressure accident scenarios, Station Blackout (SBO) and Small Break LOCA (SBLOCA), are included.

For selected bounding scenarios, the probabilistic assessments of this study are performed by outstanding framework of Two-Cell Equilibrium (TCE) /Latin Hypercubic Sampling (LHS) methodology [3,13] without any modification. TCE model predicts a DCH load considering containment cell as two cells in a conservative manner. One cell is the doner (the reactor cavity), the other is the donee (the containment atmosphere except for the reactor cavity). Since TCE includes the effects of mitigation such as the containment compartmentalization and the noncoherence of the entrainment and blowdown process, it takes on the nature of being best estimation. However DCH-specific process in TCE/LHS methodology is modeled by only the effective flow area and the coherence ratio, it is not easy to investigate the effects of complicated DCH process including entrainment of corium melt and its trapping by internal structures.

This methodology is, first of all, applied by quantifying uncertain RCS physical parameters such as molten UO_2 mass and the fraction of Zr oxidized just before vessel breach. Next, a large number of samples for these parameters are generated using LHS technique assuming conservative piecewise probabilistic distribution. And then, for each sample TCE model predicts a

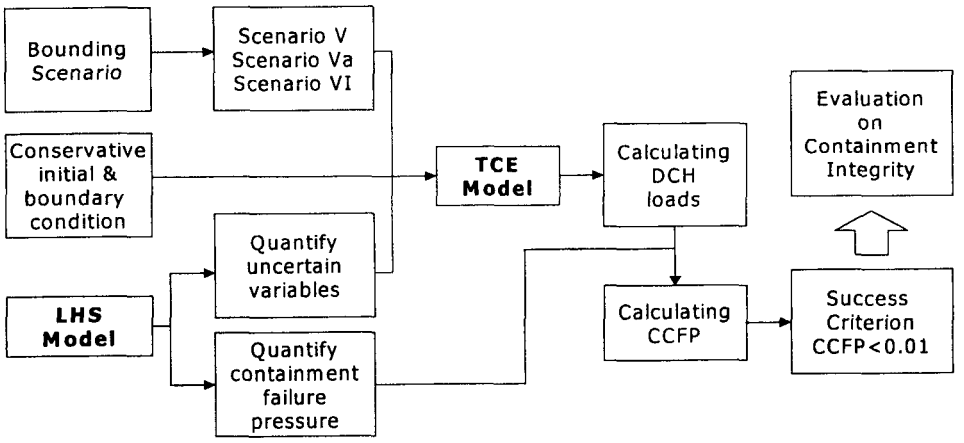

Fig. 1 A Description of TCE/LHS Methodology

DCH load where other definite initial conditions and DCH-specific modeling parameters are introduced, and finally compares with a sample of containment failure pressure from containment fragility curve. The success criterion for DCH issue resolution is that the mean conditional containment failure probability (CCFP) from the threat of early containment failure is less than 0.1. But, a tighter resolution criterion of CCFP $\leq$ 0.01, which means no more detailed analysis is required, will be applied. Fig. 1 depicts general approach of TCE/LHS methodology.

The influence of specific DCH sub-physics can be only assessed by mechanistic computer code. For the deterministic assessment, CONTAIN 2.0 code [10] with comparatively fine compartment model is used to predict detailed mechanistic responses and applied for both bounding and plant-specific accident scenarios. The required initial core melt configuration is extracted from upper limit values of the distribution functions generated for TCE/LHS assessments for bounding scenarios and MAAP4 calculation results for SBO and SBLOCA, respectively. In addition, the CONTAIN 2.0 simulations for plant-specific accident scenarios start from initial normal containment conditions, accompanying the source terms of hydrogen/steam/water mixture to be introduced into containment source compartments.

3. Quantification of Thermodynamic Conditions for HPME/DCH Analysis

3.1. Quantification of Scenario-Dependent Conditions

The initial and boundary conditions affecting the HPME/DCH phenomena can be, for convenience' sake, classified into two categories. One category is for core melts release conditions in the lower head and includes RCS temperature and pressure, core melts composition and temperature, Zr oxidation fraction, and RPV failure mechanism. These conditions are solely dependent upon the accident scenarios considered. For bounding scenarios, most probable limiting values were found in a comprehensive and systematic manner with TCE/LHS methodology guidance. Table 1 summarizes all the accident-specific conditions of KSNPs consistently applied for both deterministic and probabilistic approach.

The RCS pressures at vessel breach for Scenario

Table 1 Initial Condition for DCH Analysis

Parameter	Scenario					Parameter	Scenario				
	V	Va	VI	SBO	SB-LOCA		V	Va	VI	SBO	SB-LOCA
RCS pressure (MPa)	17.2	17.2	9	16.92	2.14	RV final hole size (m)	0.44	0.44	0.5	0.56	0.56
RCS temperature (K)	700	700	1000	755.7	618	RCS volume (m^3)	315.6	315.6	315.6	315.6	315.6
Initial pressure in containment (MPa)	0.25	0.11	0.25	0.101	0.101	Zr oxidation fraction	0.55	0.55	0.55	0.37	0.54
Initial temperature in containment (K)	400	326	400	322	322	UO_2 mass in melt (mt)	29	29	45	21.1	4.95
Initial N_2 mole fraction	0.398	0.68	0.398	0.79	0.79	ZrO_2 mass in melt (mt)	6.05	6.05	9.38	3.64	1.37
Initial O_2 mole fraction	0.106	0.196	0.106	0.21	0.21	Zr mass in melt (mt)	0.84	0.84	1.31	4.25	0.91
Initial H_2 mole fraction	0.05	0.096	0.05	-	-	Steel mass in melt (mt)	11.4	11.4	19.5	7.16	14.3
Initial steam mole fraction	0.446	0.028	0.446	-	-	Melt ejection fraction	1.0	1.0	1.0	1.0	1.0
Melt temperature (K)	2800	2800	2800	2703	2703	Cavity dispersal fraction	0.96	0.96	0.96	0.96	0.96
Total mass of UO_2 in core (mt)	85.7	85.7	85.7	85.7	85.7	Fraction of dispersed debris retained in the subcompartment*	0.62	0.62	0.62	-	-
Constant for coherence ratio*	12.2	12.2	12.2	-	-						

* These are applied for TCE/LHS assessment only.

V and Va were assumed to be at nominal overpressure set point, 17.2 MPa. For Scenario VI, it was assumed to be slightly higher than half this value, 9 MPa assuming the RCS is filled with superheated steam of 1000K. For UO_2 melt mass, recommended value [7] for CE plants of 3.13 m core diameter was used, which is slightly higher than the calculated value for KSNPs. And, the fraction of Zr oxidized ranged from 20 to 60 percent found through TCE/LHS methodology development was used, which was confirmed by plant-specific MAAP4 simulation results for SBLOCA and SBO scenarios. It should be noted, for the probabilistic parameters, that the values shown in Table 1 represent 99% of upper limiting values. For probabilistic distributions of UO_2 melt mass and Zr oxidation fraction for the TCE/LHS methodology, the same probability levels and variable intervals were applied as like earlier works. The distributions for these parameters are shown in Fig. 2 and Fig. 3, respectively. On the other hand, the mass of melt constituents except for UO_2 could be computed according to TCE/LHS methodology.

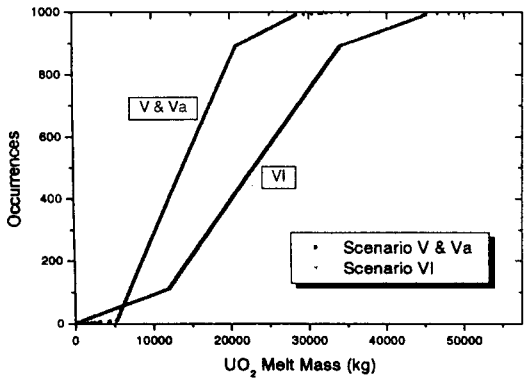

Fig. 2. Distribution of the Outcomes for UO_2 Melt Mass

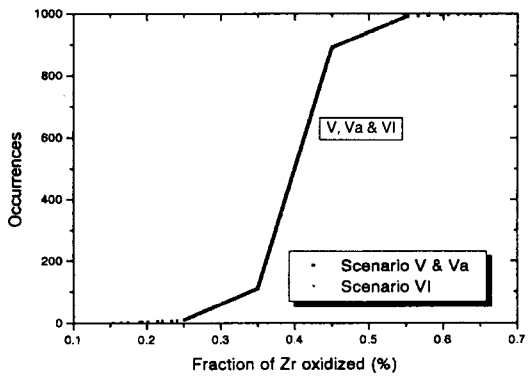

Fig. 3. Distribution of the Outcomes for Zr Oxidation Fraction

At elevated RCS pressure, most probable failure mechanism was well found to be a thermally-induced creep rupture of circumferential side of the lower head. A scaled experiment recently conducted by SNL, in which the lower head has ICI penetrations, however, showed that gross strain in the lower head induced failure of a penetration weld well before global creep rupture of the lower head would be expected [14]. And because, for DCH relevant scenarios, single massive relocation of core melt is not likely to occur and the nonuniform heating of lower head due to hot spot or quenching of corium with lower plenum water is much likely to occur, the creep rupture by side peaked heating is not likely to occur. By these reasons, we conservatively assumed RPV bottom failure of 0.4 m in diameter so that all molten material is available for ejection into the cavity. The final hole size was 0.44 m for Scenario V and Va and 0.5 m for Scenario VI, as computed with generalized ablation model [3,12]. The other category is thermodynamic conditions of the containment at vessel breach. The containment pressure at vessel breach of 0.25 MPa, if containment spray system or fan cooler is not operational (Scenario V and VI), was chosen as representative, which was confirmed as conservative by plant-specific MAAP4 calculations and many simulation results for other plants [7]. The temperature was assumed to be slightly higher than its saturation temperature (~380 K). And at atmospheric conditions given, ideal gas law with initial gas concentrations can easily calculate the gas composition at vessel breach.

For CONTAIN 2.0 simulations for SBO and SBLOCA scenarios, most of initial conditions at vessel breach were directly given by MAAP4 calculation results. Of course, general KSNPs' design data such as initial RCS and containment conditions were incorporated into MAAP4 parameter file [13]. The predicted values for major parameters are also summarized in Table 1. It can be seen that although the parameters are sensitive to accident scenarios, most of them are bounded below the values from bounding scenarios.

3.2. Quantification of the DCH Phenomena

The parameters related to DCH phenomena are classified in the following time order: the amount of ejected core melt, the fraction of debris dispersal, coherence ratio, and debris transport fractions depending upon pathways from the reactor to the containment dome. Among them,

the common parameters for probabilistic and deterministic assessments are also summarized in Table 1.

For an amount of ejected material to participate in DCH process, a conservative upper bound of 100 percent was used for all the scenarios in this study. Although the fraction of debris dispersal from the reactor cavity is likely to be less than unity since it is expected for some retention by freezing on cavity surfaces, conservative value of 0.96 was used [7]. The coherence ratio, which is defined as the ratio of the characteristic dispersal time to the characteristic time constant for steam blowdown, is expressed as: [3]

$$R_r = \frac{\tau_e}{\tau_b} = C_{Rt} f_{disp} \left(\frac{T^0_{RCS}}{T^0_d} \right)^{1/4} \left(C_{d,h} \frac{M^0_d}{M^0_g} \frac{A_h V_c^{1/3}}{V_{RCS}} \right)^{1/2} \quad (1)$$

where C_{Rt} is a constant that is determined from experimental data.

This parameter relates the complexity of the reactor cavity configuration with debris/gas interactions during debris dispersal process. But since this parameter is considered as a weak function of plant geometry, the reactor cavity configurations for this can be categorized as IDCOR categorization of 3 groups, which are Zion-like, Surry-like, and others by US NRC' s DCH study. Fig. 4 shows a schematic of KSNP' s cavity configuration of U-type from the reactor cavity vessel to the ICI Chase. KSNP' s cavity configuration can be categorized as a Surry-like cavity type. It means that the constant (C_{Rt}) for coherence ratio about KSNP' s cavity in TCE/LHS assessment is 12.2, which is that about the Surry-like type cavity [6]. Whereas TCE models internally computes the coherence ratio by Eq. (1) with this constant, this parameter has to be adjusted in the CONTAIN 2.0 assessment by modeling steam blowdown and the entrainment of ejected melt material, for which the method will be discussed in Section 4.2 in greater detail.

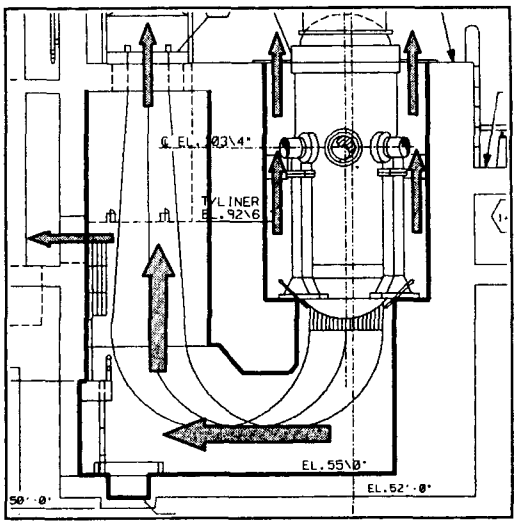

Fig. 4. The Schematic of the KSNP Reactor Cavity and Its Surroundings

On the other hand, some of the debris dispersed from the cavity can introduce into the compartments of the containment outer walls through any of possible flow paths. In KSNPs, there are two primary debris transport pathways; the annular gap between the RPV and the biological shield wall and manways leading into the lower compartments through the in-core instrument (ICI) tunnel. In more detail, pathways available for debris dispersal from the cavity to other compartments are summarized in Table 2. Of these paths, Paths 1 and 3 are directed into the containment dome and were applied to TCE/LHS assessments. Based on minimum flow area of those pathways, it was calculated that 38% of the debris that was dispersed could be carried over into the containment dome. In CONTAIN 2.0 modeling, all the possible pathways were considered as engineered vent paths. Fig. 5 is a schematic of simple containment nodalization of 8 compartments, in which the number of compartments was minimized as much as possible for the closer

Table 2 Debris Transport Pathways from the Reactor Cavity

Path	Description	Minimum Flow Area (m^2)
1	Flow through the ICI tunnel and chase past the failed seal table, and out into the upper compartment. If the seal table does not fail this flow path is not viable	3.26
2	Upward flow, through the reactor vessel biological shield annulus, out through the hot/cold leg biological shield penetrations, and out into the lower compartments.	12.44
3	Upward flow, through the reactor vessel biological shield annulus, past the vessel flange and out into the upper compartment.	2.56
4	Flow through the ICI tunnel/chase through the chase doorway (man-way entrance) and out into the lower compartment.	1.95
5	Flow through the ICI tunnel/chase through the lower compartment.	1.31

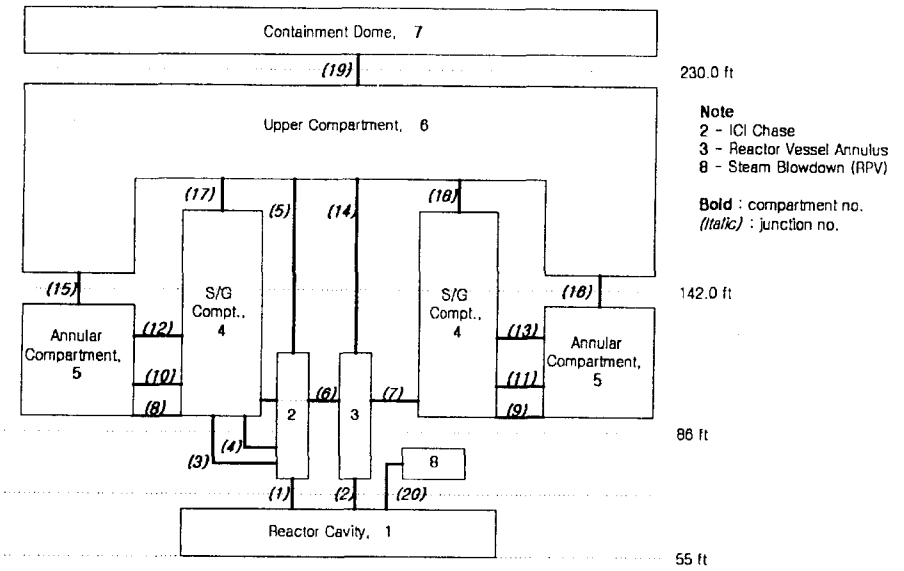

Fig. 5. The Containment Nodalization for CONTAIN2.0 Analyses

simulation to TCE/LHS assessment and to avoid the artificial mixing between the compartments. To appropriately simulate the debris transport to the containment dome, however, the neighbors of reactor cavity area were separated into 3 compartments: ICI tunnel, RPV annulus, and lower compartment. Therefore, CONTAIN 2.0 calculates the fraction of the debris to carry over the containment dome by mechanistic flow model imposed by the flow resistances. The primary system cell was artificially created to simulate the steam blowdown in which the primary system (cell no. 8) initially had RCS condition at vessel breach.

4. Calculation Results

4.1. TCE/LHS Assessments

The LHS runs produced outcomes of 1000 samples for predescribed distributions of uncertain parameters for three bounding scenarios. During this process, sampling values of containment failure pressure were also generated with the containment fragility curve [15]. Fig. 2 and 3 show the cumulative distributions of molten UO_2 mass in the lower head at vessel breach and Zr oxidation fraction as a result of LHS runs, which are generated by rearranging the outcomes at the ascending order. The data corresponding to 990 occurrences, are well agreed with the values described in Table 1, which confirms that a number of sampling for the assessment was appropriate.

The containment loads were calculated using TCE model for each LHS outcome. Whereas the TCE runs produce the distributions of final RPV failure size, coherence ratio, and containment temperature, the final output of TCE runs is CCFP. The CCFP is calculated by counting the occurrence of the containment load exceeding the containment failure pressure. The calculated CCFPs of all the scenarios were zero, which means that it is expected that for all the accident scenarios the maximum pressure load induced by DCH is lower than the containment failure pressure obtained from the fragility curve. Thus, it can be stated that the KSNP containment is robust to the DCH threat.

On the other hand, Fig. 6 showed calculation results of TCE runs, in which containment pressure was represented as a function of cumulative probability. The 99% upper bounding values of DCH loads were 0.537, 0.605, and 0.758 MPa for Scenario V, Va, and VI, respectively. The reason that pressure load for

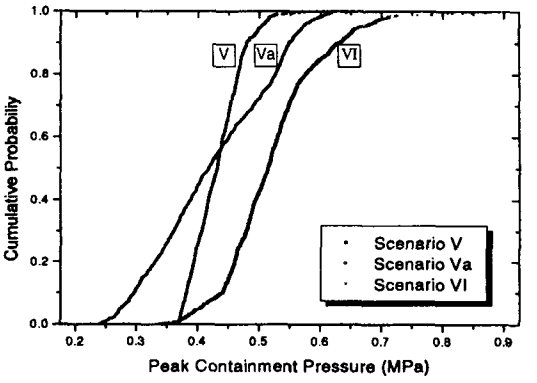

Fig. 6. Estimated Peak Containment Pressures from TCE/LHS Calculation

Scenario VI was much higher is not obvious since TCE model could not give a detail of DCH consequence. Whereas the DCH loads could be influenced by the DCH-induced chemical reaction and hydrogen combustion as well as DCH debris/gas heat transfer, it was likely that the larger core melt in Scenario VI dominantly contributed on containment load.

4.2 CONTAIN 2.0 Calculations

4.2.1. Bounding Accident Scenarios

CONTAIN 2.0 evaluations require troublesome modelings for many different DCH processes. Lack as technical modeling on the plant application is, CONTAIN 2.0 User's Manual can give good guidance for this work [10]. Table 3 summarizes the DCH modeling developed for this study. Among the processes seen in Table 3, core melt ejected from RPV and cavity dispersal fraction was already determined in Section 3.1 and can be easily introduced into CONTAIN 2.0 grammatical context. Instead, the modeling of cavity entrainment rates accompanied by steam blowdown is somewhat difficult and can be performed by defining steam blowdown interval

Table 3 The Parameter Description for CONTAIN2.0 Modeling

	Parameter description	Scenario V	Scenario Va	Scenario VI	SBO	SBLOCA
RPV Blowdown	The steam mass in the RCS at vessel breach (kg)	17,000	17,000	6,000	15,300	2,360
	An interval of blowdown duration (sec)	2.0735	2.0735	2.1842	2.083	5.84
	Final lower head hole diameter (m)	0.435	0.435	0.500	0.559	0.276
Debris Sources	Initial trapped debris mass in the reactor cavity (kg)	48,552	48,552	79,071	36,156	21,507
	Debris mass to be entrained from the reactor cavity (kg)	46,610	46,610	75,908	34,536	20,646
	Start time of the entrainment from steam blowdown (sec)	0.518	0.518	0.546	0.521	1.461
	End time of the entrainment from steam blowdown (sec)	3.3	3.3	6.1	3.7	3.6
Debris Slip Ratio		5 in cavity and connecting cells, 1 elsewhere				
Trapping Model	Type	None in cavity and connecting cells, TOF/KU elsewhere				
	The first trapping length	Length from flow path exit to first structure in the cell				
	The second trapping length	6Vg/Sstr where Vg is cell gas volume and Sstr is total surface area in the cell				
	The third trapping length & the gravitational height	Cell height				

and then relating this with coherence ratio. Fig. 7 explains the relationship between the steam blowdown and melts entrainment. The steam blowdown was calculated by opening a flow path (flow path no. 16 in Fig. 5) from the primary system to the compartment representing the reactor cavity, in which the flow area was linearly increased with time over an interval of duration. The duration of blowdown interval was given by the semi-empirical relation [16]

$$\tau_h = 0.4 \cdot \left(\frac{S}{0.1}\right) \cdot \left(\frac{0.4}{d_h / S}\right)^2 \cdot \sqrt{\frac{6.3}{P^0_{RPV}}} \qquad (2)$$

where τ_h is in seconds, d_h is the final value of the reactor vessel failure size in meters, P^0_{RPV} is the pressure in the RPV in MPa at the start of blowdown, and S is the geometric linear scale factor, i.e., S=1 for this analysis. In principle, the pressure P^0_{RPV} should be corrected for the decrease in pressure corresponding to the increase in RPV free volume that results from ejection of the melt. This correction is given by

$$P^0_{RPV} = P_{RPV,VB} \cdot \left(1 - \frac{V_{melt}}{V_{RCS}}\right)^{\gamma} \qquad (3)$$

where isentropic depressurization is assumed, $P_{RPV,VB}$ is the pressure at vessel breach prior to melt ejection, V_{melt} is the volume of the melt, V_{RCS} is the RCS volume, and γ is the ratio of specific heats (1.33 for steam). For KSNPs, τ_h was found to be 2.074 seconds for Scenario V and Va, and 2.184 seconds for Scenario VI. During these time intervals, the

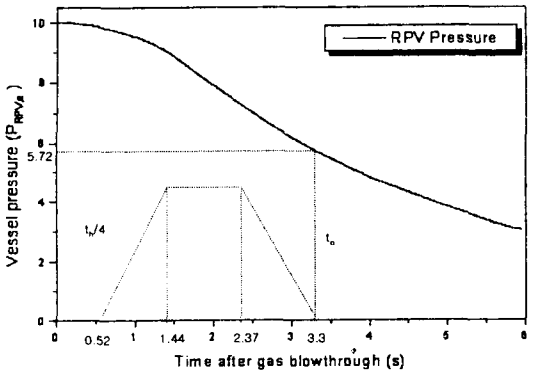

Fig. 7. Schematic of Approach for Defining RPV Blowdown and Airborne Debris Sources in DCH Calculations (Scenario V)

blowdown flow paths opened from 0.4 m to corresponding final size, 0.435 m for Scenario V and Va, and 0.5 m for Scenario VI, respectively.

In order to calculate the interval of entrainment duration, the RPV pressure at the end of the entrainment interval was estimated by the following relation, where the coherence ratio predetermined by TCE/LHS assessments was applied.

$$R_t = \frac{2}{\gamma - 1}\left[\left(\frac{P^0_{RPV}}{P_{RPV,e}}\right)^{\frac{\gamma-1}{2\gamma}} - 1\right] \quad (4)$$

And, the end time of debris entrainment could be determined from the steam blowdown curve with $P_{RPV,e}$. It was estimated to be 3.3 seconds for Scenario V and Va, 6.1 seconds for Scenario VI. For all these data, the entrainment rate of core melt dispersed from the reactor cavity was finally estimated with the prescription provided by Reference 10, which is also depicted in Fig. 7. The values corresponding to height of trapezoidal shape for UO_2 mass were found to be about 15.0 mt for Scenario V and Va, and 11.7 mt for Scenario VI, respectively.

For debris transport and trapping, the slip parameters s = 5 for all debris fields for the reactor cavity and the directly connected compartments and s = 1 elsewhere were specified. Trapping in the cavity and connected compartments was not modeled because the effects of any trapping in these regions had been already taken account into in the dispersal fraction. And, the time-of-flight/Kutateladze number (TOF/KU) trapping model was used. Recommended values for plant applications were applied for all the other parameters.

The CONTAIN 2.0 calculation results for the peak pressures were represented in Fig. 8 and Fig. 9 for two compartments. In the reactor cavity,

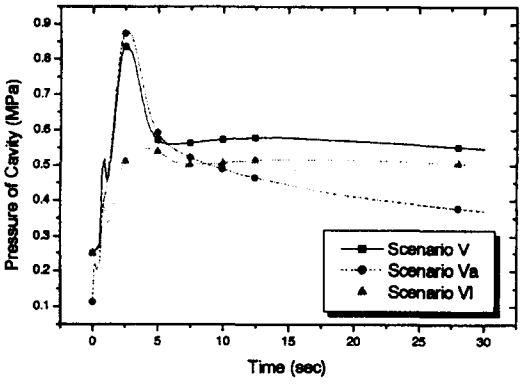

Fig. 8. Distribution of Pressures in the Reactor Cavity (CONTAIN 2.0 calculations)

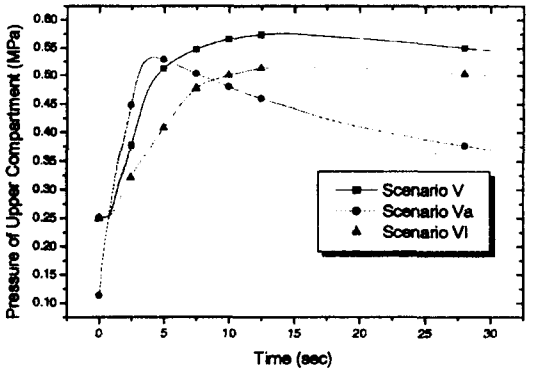

Fig. 9. Distribution of Pressures in the Upper Compartment (CONTAIN 2.0 calculations)

initially pressure peaks have appeared due to high-pressure steam blowdown inducing high-temperature airborne debris generation. The peak pressures are 0.836 MPa for Scenario V, 0.876 MPa for Scenario Va, and 0.547 MPa for Scenario VI, respectively, as can be seen in Fig. 8. As the high temperature debris was dispersed from the reactor cavity through flow paths, the pressures in the containment atmosphere rose rapidly with a time delay of about 3 to 10 seconds. And then, the pressure transients starting from the reactor cavity have diminished and arrived at equilibrium between all the compartments within 15 seconds at most. Finally, the pressures have decreased gradually due to heat losses to the surrounding heat structures, or sustained by continuous DCH-induced hydrogen combustion. The maximum DCH loads in containment were estimated to be 0.576, 0.533, and 0.515 MPa for Scenario V, Va, and VI, respectively, as seen in Fig. 9.

It is noted that the pressure history following the transients is governed by DCH-induced hydrogen combustion. Scenario V and VI have relatively inflammable gas mixture at initial containment atmosphere (for gas mixture, see Table 1) so that initial peaks in reactor cavity and ongoing pressure rises in containment are resulted from DCH phenomena itself accompanied by the steam blowdown. The relative magnitude of pressure peaks depends upon initial RCS pressure at vessel breach. After the equilibrium, constantly sustaining pressures for these scenarios are resulted from continuous hydrogen burning. This fact could be confirmed by Fig. 10, which represents cumulative mass of hydrogen burned in the upper compartment. In Scenario Va, because initial gas mixture is very sensitive to hydrogen combustion a large amount of hydrogen continuously burns even within the DCH time scale, i.e. 5 seconds. This result can be also seen in Fig. 10. Augmented by this burning, therefore, initial peak pressures in Scenario Va are the highest among the accident scenarios analyzed. But, after all the hydrogen is consumed, the pressure decreases due to heat losses to the surrounding heat structures.

The entrained mass of the melt during DCH process is shown as Fig. 11, which realizes the effect of the geometrical configurations on DCH loads. This quantity, defined as time-dependent mass retained in the containment atmosphere, reflects trapped debris mass between various compartments. Because the primary system pressure of Scenario VI was lower than those of other scenarios, more parts of the debris was trapped in lower compartments before they reached to upper compartment. For Scenario V, 60.1% among total amount of melt debris was only trapped lower compartments, but 71.3% was trapped in Scenario VI. These results are expected to be similar, compared with TCE/LHS calculations (62%).

4.2.2. High-Pressure Accident Scenarios

The DCH loads resulting from SBO and SBLOCA as typical plant-specific high-pressure accident scenarios were also estimated to verify that the assessments for bounding accident scenarios could be conservative. The thermodynamic responses of RCS and the containment before vessel breach were predicted using the MAAP4 code. However, information about the RCS effluents into the containment and the properties of thermo-hydraulic material including core melt was only implemented into CONTAIN 2.0 analyses. Major parameters from full time-scale simulations for two scenarios are summarized in Tables 1 and 3. It can be seen that although the parameters are sensitive to accident scenarios, most of them are bounded below the values from bounding scenarios. Fig. 12 and Fig.

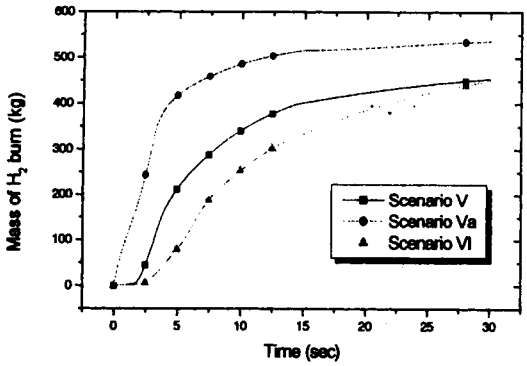

Fig. 10. Distribution of Mass of Hydrogen Burn in the Upper Compartment (CONTAIN2.0 Calculations)

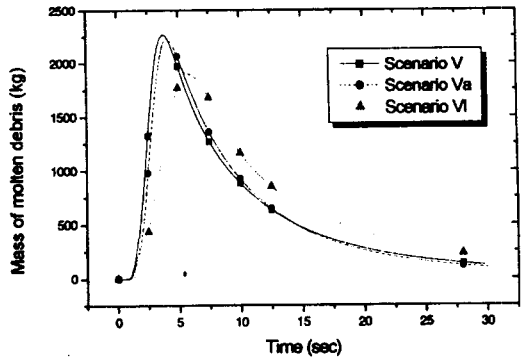

Fig. 11. Distribution of Mass of Debris in the Upper Compartment (CONTAIN2.0 calculations)

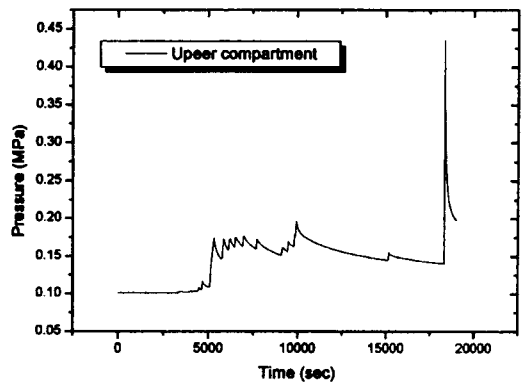

Fig. 12. Pressure in the Containment for SBO Scenario (CONTAIN 2.0 Calculation)

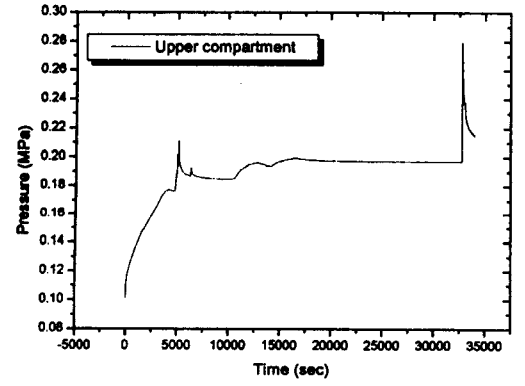

Fig. 13. Pressure in the Containment for SBLOCA Scenario (CONTAIN 2.0 Calculation)

13 show the predicted pressure histories at various compartments in which the pressure distribution of the containment compartments was well uniform. Compared with the largest peak, the smaller ones resulted from sources of water/steam/H_2 released into the containment before vessel breach could be ignored. The largest peaks seen in these figures can be easily understood as DCH loads accompanying by the reactor vessel failure: the reactor vessel failure occurred at 18,314 sec for SBO and 32,744 sec for SBLOCA, respectively. The instantaneous peak pressures in upper compartments were estimated to be 0.435 and 0.279 MPa, respectively. These results showed lower loads than those of Scenario V, Va , and VI because of smaller amount of melts, smaller amount of hydrogen burning, lower pressure and temperature in the primary system at vessel breach time, and initial conditions in containment.

To assess the effects of DCH phenomenological parameters on containment loads, the sensitivity calculations for SBO accident were performed. The parameters include the amount of core melts, the existence of co-ejected primary system water,

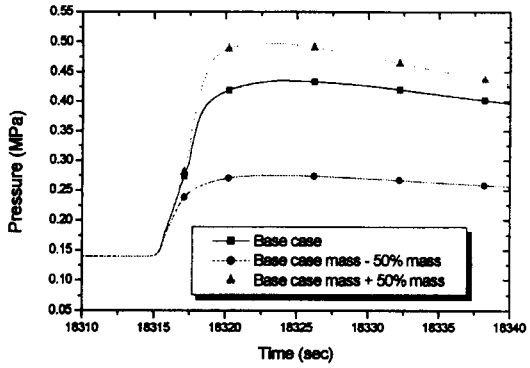

Fig. 14. The Sensitivity Calculations for the Amount of the Melts

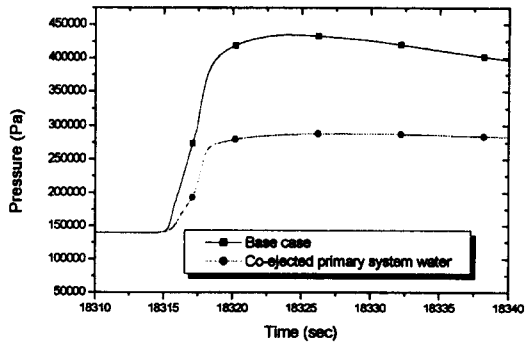

Fig. 15. The Sensitivity Calculations for the Co-ejected Primary System Water Option

coherence ratio, and debris size and distribution. These analyses showed that DCH loads were strongly dependent on the amount of melts if the HPME happened under maximum steam blowdown pressure, as seen in Fig. 14. When core melt mass increased 50% from base case, the maximum DCH load increased 0.5 MPa from 0.435 MPa. Co-ejected primary system water was considered to be mitigation factor of DCH phenomena (Fig. 15). Other parameters such as coherence ratio and debris/gas heat transfer showed some influence on the DCH phenomena, but did not affect maximum DCH load. Considering these parameters at the same time, effects of the factors increasing the DCH load could be compensated for by ones decreasing the load.

5. Conclusions

As a process of DCH issue resolution for KSNPs, a containment load/strength assessment with two different approaches, the probabilistic and the deterministic, was performed with all plant-specific and phenomena-specific data. For three bounding scenarios, the calculation results of TCE/LHS and CONTAIN 2.0 with the conservatism or typical estimation for uncertain parameters, showed that the containment failure resulted from DCH was not likely to occur. The CONTAIN 2.0 calculations for plant-specific high-pressure scenarios including the sensitivity calculations for DCH phenomenological parameters, also has confirmed that the predicted containment pressure and temperature were much below those from these two approaches. Although it could not help refining the DCH phenomenological parameters, it can be, therefore, concluded that DCH issue for KSNPs might be not a problem.

6. Acknowledgement

This work was performed under the financial support of Korea Institute of Nuclear Safety. The authors express their grateful thanks to Se-Won Lee and Hee-Jin Ko, KOPEC for their continuous encouragement and support.

7. References

1. SECY-93-087, "Policy, Technical, and Licensing Issues Pertaining to Evolutionary and Advanced Light-Water Reactor (LWR) Designs," USNRC, April, 2, (1993).
2. KURD, " Korean Utility Requirements

Document, Chapter 5: Engineered Safety Systems," Rev. 0, KEPCO, June, (1998).
3. M.M.Pilch, et al., "The Probability of Containment Failure by Direct Containment Heating in Zion," NUREG/CR-6075, SAND93-1535, Sandia National Laboratories, December, (1994).
4. M.M.Pilch, et al., "The Probability of Containment Failure by Direct Containment Heating in Zion," NUREG/CR-6075 Supplement 1, SAND93-1535, Sandia National Laboratories, December, (1994).
5. M.M.Pilch, et al., "The Probability of Containment Failure by Direct Containment Heating in Surry," NUREG/CR-6109, SAND93-2078, Sandia National Laboratories, May, (1995).
6. M.M.Pilch, et al., "Resolution of the Direct Containment Heating Issue for All Westinghouse Plants with Large Dry Containments or Subatmospheric Containments," NUREG/CR-6338, SAND95-2381, Sandia National Laboratories, February (1996).
7. M.M.Pilch, et al., "Resolution of the Direct Containment Heating Issue for Combustion Engineering Plants and Babcock & Wilcox Plants," NUREG/CR-6475, SAND97-0667, Sandia National Laboratories, November (1998).
8. S.B.Kim, et al., "Evaluation of the Containment Integrity due to Direct Containment Heating in Korean 1300 MWe PWR," Korea Atomic Energy Research Institute, Transactions of the 15th International Conference on Structural Mechanics in Reactor Technology (SMiRT-15), Section XI, pp. 197-205, Seoul, Korea, August 15-20, (1999).
9. K.K.Murata, et al., "Code Manual for CONTAIN 1.2: A Computer Code for Nuclear Reactor Containment Analysis," (Draft), Sandia National Laboratories, April, (1993).
10. K.K.Murata, et al., "Code Manual for CONTAIN 2.0: A Computer Code for Nuclear Reactor Containment Analysis," NUREG/CR-6533, SAND97-1735, Rev. 0, Sandia National Laboratories, June, (1997).
11. J.W.Park, et al., "Estimation of Direct Containment Heating Loads in KNGR Using CONTAIN Code," Korea Power Engineering Company, Inc., Presented at the 1999 KNS Spring Meeting, (CD-ROM), Pohang, Korea, May, (1999).
12. Henry, R. E. et al., "MAAP4-Modular Accident Analysis program for LWR Power Plants," EPRI, May (1994).
13. R.L.Iman and M.J.Shortencarier, "A FORTRAN 77 Program and User's Guide for the Generation of Latin Hypercube and Random Samples for Use with Computer Models," NUREG/CR-3624, SAND83-2365, Sandia National Laboratories, March, (1984).
14. T.Y.Chu, et al., "An Assessment of the Effects of Heat Flux Distribution and Penetration on the Creep Rupture of a Reactor Vessel Lower Head," Twelfth Proceedings of Nuclear Thermal Hydraulics, 1997 ANS Annual Winter Meeting, pp. 135-144, Albuquerque, November, (1997).
15. KEPCO, "Ulchin Unit 3&4 Final Probabilistic Safety Assessment Report," vol. 5.
16. D.C.Williams, et al, "CONTAIN Code Analyses of Direct Containment Heating (DCH) Experiments: Model Assessment and Phenomenological Interpretation," Proceedings of the ANS Winter Meeting, Thermal Hydraulics Division, pp. 495-497, San Francisco, October, (1995).